USGS
science for a changing world

Prepared in cooperation with the U.S. Fish and Wildlife Service

Model Structure of the Stream Salmonid Simulator (S3)—A Dynamic Model for Simulating Growth, Movement, and Survival of Juvenile Salmonids

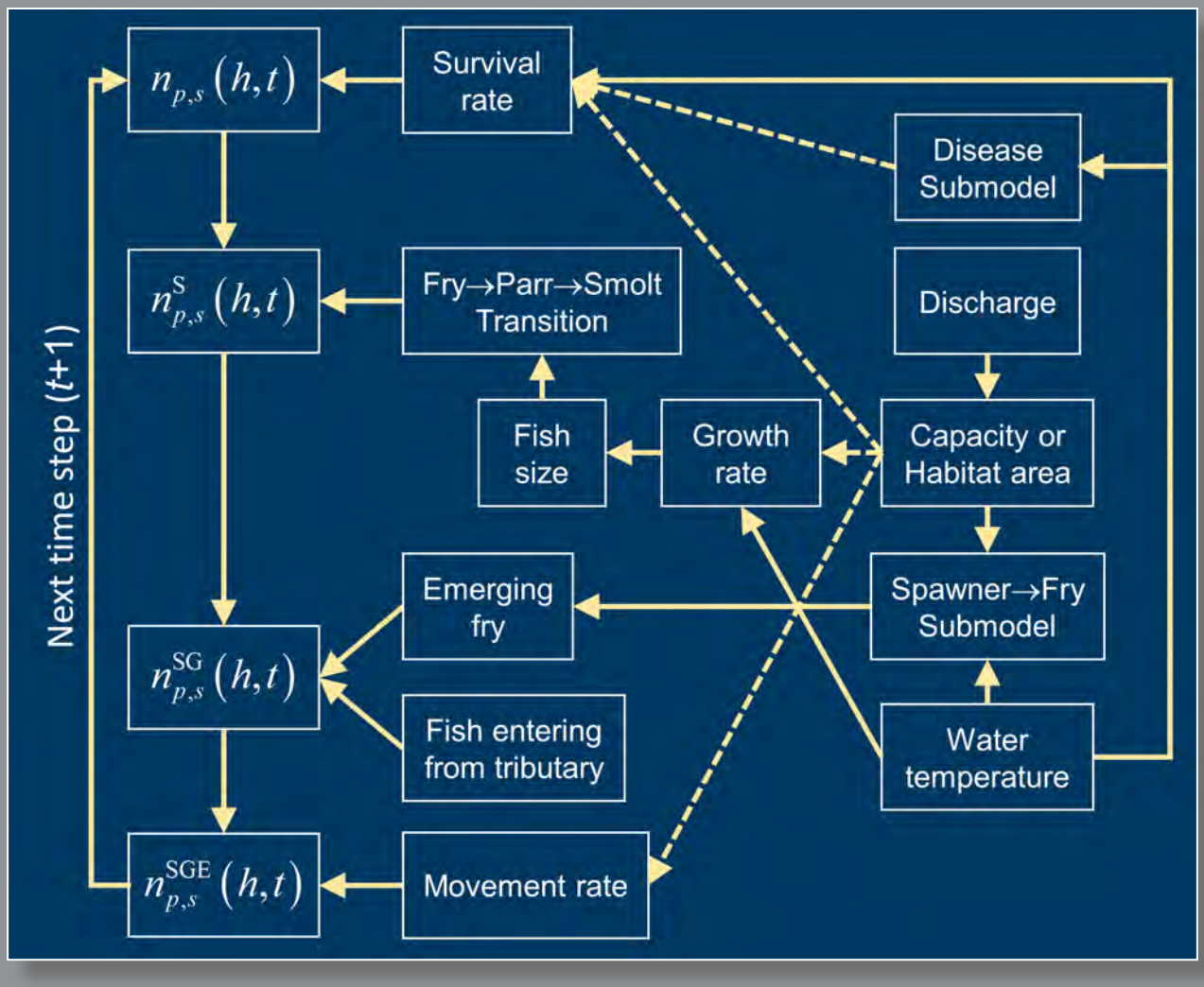

Open-File Report 2018-1056

U.S. Department of the Interior
U.S. Geological Survey

Cover: Schematic summary of the Stream Salmonid Simulator (S3) model showing linkages between physical drivers, demographic processes, and changes in daily abundance. Dashed lines show submodels that that may be turned on or off to represent different dynamic processes in the S3 model.

Model Structure of the Stream Salmonid Simulator (S3)—A Dynamic Model for Simulating Growth, Movement, and Survival of Juvenile Salmonids

By Russell W. Perry, John M. Plumb, Edward C. Jones, Nicholas A. Som, Nicholas J. Hetrick, and Thomas B. Hardy

Prepared in cooperation with the U.S. Fish and Wildlife Service

Open File Report 2018–1056

U.S. Department of the Interior
U.S. Geological Survey

U.S. Department of the Interior
RYAN K. ZINKE, Secretary

U.S. Geological Survey
William H. Werkheiser, Deputy Director
exercising the authority of the Director

U.S. Geological Survey, Reston, Virginia: 2018

Suggested citation:
Perry, R.W., Plumb, J.M., Jones, E.C., Som, N.A., Hetrick, N.J., and Hardy, T.B., 2018, Model structure of the stream salmonid simulator (S3)—A dynamic model for simulating growth, movement, and survival of juvenile salmonids: U.S. Geological Survey Open-File Report 2018-1056, 32 p., https://doi.org/10.3133/ofr20181056.

ISSN 2331-1258 (online)

Contents

Figures

Tables

Conversion Factors

U.S. customary units to International System of Units

Multiply	By	To obtain
	Flow rate	
cubic foot per second (ft^3/s)	0.02832	cubic meter per second (m^3/s)

International System of Units to U.S. customary units

Multiply	By	To obtain
	Length	
millimeter (mm)	0.03937	inch (in.)
kilometer (km)	0.6214	mile (mi)
	Area	
square meter (m^2)	10.76	square foot (ft^2)
	Migration rate	
kilometer per day (km/d)	0.6214	mile per day (mi/d)
	Diffusion rate	
square kilometer per day (km^2/d)	0.3861	square mile per day (m^2/d)
	Mass	
gram (g)	0.03527	ounce, avoirdupois (oz)
kilogram (kg)	2.205	pound avoirdupois (lb)

Temperature in degrees Celsius (°C) may be converted to degrees Fahrenheit (°F) as follows:
°F=(1.8×°C)+32

Abbreviations

HSC	habitat suitability criteria
WUA	weighted usable area
S3	Stream Salmonid Simulator
2D	two-dimensional

Model Structure of the Stream Salmonid Simulator (S3)—A Dynamic Model for Simulating Growth, Movement, and Survival of Juvenile Salmonids

By Russell W. Perry[1], John M. Plumb[1], Edward C. Jones[1], Nicholas A. Som[2], Nicholas J. Hetrick[2], and Thomas B. Hardy[3]

Abstract

Fisheries and water managers often use population models to aid in understanding the effect of alternative water management or restoration actions on anadromous fish populations. We developed the Stream Salmonid Simulator (S3) to help resource managers evaluate the effect of management alternatives on juvenile salmonid populations. S3 is a deterministic stage-structured population model that tracks daily growth, movement, and survival of juvenile salmon. A key theme of the model is that river flow affects habitat availability and capacity, which in turn drives density dependent population dynamics. To explicitly link population dynamics to habitat quality and quantity, the river environment is constructed as a one-dimensional series of linked habitat units, each of which has an associated daily time series of discharge, water temperature, and usable habitat area or carrying capacity. The physical characteristics of each habitat unit and the number of fish occupying each unit, in turn, drive survival and growth within each habitat unit and movement of fish among habitat units.

The purpose of this report is to outline the underlying general structure of the S3 model that is common among different applications of the model. We have developed applications of the S3 model for juvenile fall Chinook salmon (*Oncorhynchus tshawytscha*) in the lower Klamath River. Thus, this report is a companion to current application of the S3 model to the Trinity River (in review). The general S3 model structure provides a biological and physical framework for the salmonid freshwater life cycle. This framework captures important demographics of juvenile salmonids aimed at translating management alternatives into simulated population responses. Although the S3 model is built on this common framework, the model has been constructed to allow much flexibility in application of the model to specific river systems. The ability for practitioners to include system-specific information for the physical stream structure, survival, growth, and movement processes ensures that simulations provide results that are relevant to the questions asked about the population under study.

[1]U.S. Geological Survey.
[2]U.S. Fish and Wildlife Service.
[3]Texas State University, San Marcos, Texas.

Introduction

Many anadromous salmonid populations along the West Coast of North America have declined substantially over the past century owing partly to construction of dams for flood control, hydroelectricity, and domestic and agricultural water. In river systems that support anadromous salmonid populations, flow regulation can influence water quality; water temperature; and the magnitude, timing, and variability of daily discharge. These alterations to the river environment, in turn, influence the productivity of anadromous salmonid populations. Thus, water management in regulated river systems often seeks to balance human uses of water with maintenance and recovery of anadromous salmonid populations.

Fisheries and water managers often use population models to aid in understanding the effect of alternative water management or restoration actions on anadromous fish populations. Salmon population models are diverse, ranging from coarse-grained statistical stock-recruitment models that encompass the entire life cycle (Salmon Technical Team, 2005) to detailed agent-based models that track individual fish on fine temporal scales (for example, daily) in two spatial dimensions (Railsback and others, 2013). Diversity in the structure and detail built into a population model stems from the particular goals and questions that the modeling effort aims to answer. Population models are built and used to answer specific types of management questions. These questions should ultimately drive the optimal spatial, temporal, and biological structure of the population model (Rose and others, 2011).

The operation of impassable dams influences downstream populations of Chinook salmon (*Oncorhynchus tshawytscha*), coho salmon (*Oncorhynchus kisutch*), and steelhead (*Oncorhynchus mykiss*) in the lower Klamath and lower Trinity Rivers. Consequently, resource managers for the Klamath and Trinity Rivers have long relied on detailed habitat and population models to aid in understanding effects of management actions on salmon populations (Williamson and others, 1993; Bartholow, 1996; Hardy and others, 2006). In these river basins, general questions relating to water and fish management include the following:

- How does management of daily river flows affect production of juvenile salmon in reaches downstream of the dam?
- How do daily dam operations influence habitat quantity and quality, and, in turn, affect juvenile salmon movement, growth, and survival?
- How does disease caused by *Ceratomyxa shasta*, a myxozoan parasite, influence infection and mortality of juvenile salmon?
- How do past, present, and future habitat restoration alternatives influence juvenile salmon production?
- How can water temperatures best be managed to minimize mortality and maximize growth of juvenile salmon?

Although potential management alternatives often are much more specific, these general questions help to guide the design of a population model intended to inform management alternatives.

To provide resource managers with a tool for understanding how various management actions affect juvenile salmon populations, we developed the Stream Salmonid Simulator (S3), a dynamic simulation model that mimics growth, movement, and survival of juvenile salmonid populations in streams and rivers. The S3 model is based in concept on SALMOD, a fish production model with a long history in the Klamath Basin (Bartholow and others, 1993; Williamson and others, 1993; Bartholow, 1996; Bartholow and others, 2002). The underlying basis of SALMOD is that daily flows influence the amount of habitat available to different salmonid life stages, and the amount of habitat influences density-dependent processes that affect fish production. In developing S3, our goal was to retain the essential ideas behind SALMOD (linking fish habitat to production), but to reinvent the modeling framework to:

- Develop a more rigorous mathematical basis for spatially explicit population dynamics in a riverine environment,
- Update movement models to incorporate recent advances in modeling juvenile salmon migration,
- Implement more mechanistic growth models parameterized for anadromous salmonids of interest, and
- Implement the model in an open-source modeling platform.

To explicitly link population dynamics to habitat quality and quantity in the S3 model, the river environment is constructed as a one-dimensional series of linked habitat units, each of which has an associated daily time series of discharge, water temperature, and usable habitat area or carrying capacity. The physical characteristics of each habitat unit and the number of fish occupying each unit, in turn, are used to drive survival and growth within each habitat unit and movement of fish among habitat units. The model runs on a daily time step because (1) daily flows and water temperatures often are the subject of water management; and (2) juvenile salmon growth, movement, and survival depend on how water flow, habitat, and temperature evolve over time. S3 is a stage-structured model, allowing demographic rates to differ among life stages of eggs, fry, parr, and smolts. Furthermore, the model can track different population segments separately (for example, by species, run-type, tributary origin, or rearing origin), thereby providing an understanding of how different population segments respond to the environment. Because juvenile salmon production depends not only on the quantity of fish produced but the quality of fish produced as measured by their size, we explicitly model growth rates of juveniles salmon. Growth rates affect fish size, which in turn determines when fish transition from one life stage to the next.

Our goal was to build a simulation model that was general enough to capture essential population dynamics in a “generic” river with anadromous salmonids, but specific enough that the model could be adapted with relatively little effort to answer specific questions for a given watershed. With this goal in mind, the purpose of this report is to outline the underlying general structure of the S3 model that is common among different applications of the model. We have developed two applications of the S3 model that are described in two forthcoming companion USGS reports—one for juvenile fall Chinook salmon in the lower Klamath River and one for juvenile fall and spring Chinook salmon on the lower Trinity River. In this report, we detail model structure that is common to both applications, whereas specific detail on model construction, data sources for model inputs, parameterization, and model calibration are provided in the two companion reports (Perry, USGS, written oral comm, 2018). Furthermore, although the framework of S3 is generalized for any anadromous salmonid species, in this report we present submodels (for example, growth) parameterized for Chinook salmon to support current applications to Chinook salmon in the Klamath and Trinity Rivers.

Methods

General Model Structure for Survival, Life Stage Transitions, and Movement

The heart of the S3 model is the dynamic simulation of growth, movement, and survival of juvenile salmon during riverine rearing. The S3 model tracks the number of individuals by habitat unit, date, life stage, and source population. Formally, we define this quantity as $n_{p,s}(h, t)$ where:

n = number of individuals;

p = source population, $p = 1, \ldots, P$;

s = life stage, s = eggs, fry, parr, or smolt, for example;

h = habitat unit, $h = 1, \ldots, H$; and

t = day (or date), $t = 1, \ldots, T$.

As this notation implies, S3 is a discrete-space, discrete-time model that runs on a daily time step. We mix scripting notation here to distinguish the fundamental spatiotemporal model and data structure from the different population components that form population structure. Thus, parenthetical notation using (h, t) stresses a matrix formulation where each population component has an associated abundance with habitat units forming matrix rows and time (dates) form matrix columns. In contrast, subscript notation distinguishes each H by T abundance matrix for particular population components consisting of either life stage (s) or source population (p).

Spatially, the continuous longitudinal axis of the river is divided into a series of discrete spatial units of length $\Delta x_h = x_{h,\text{up}} - x_{h,\text{down}}$, where x is the distance (in kilometers) from the downstream terminus of the model domain (typically the mouth of the river) and $x_{h,\text{up}}$ and $x_{h,\text{down}}$ mark the upstream and downstream boundaries of habitat unit h. Although we generally refer to these discrete spatial segments as "habitat units", this framework allows complete flexibility in defining the physical habitat template of the model. For example, the river may be divided into a series of fixed-length reaches (for example, every kilometer) or discretized based on varying-length meso-habitat units such as runs, riffles, and pools. Each habitat unit is associated with a time series of physical habitat characteristics that may be used to drive population dynamics. For example, each habitat unit has an associated time series of discharge, water temperature, amount of usable habitat (in square meters), or habitat capacity (number of fish) for each life stage.

Source populations (p) represent characteristics of groups entering the domain of the model that the user wishes to track. The model can simultaneously track distinct populations based on rearing origin (for example, hatchery, wild origin), species (for example, Chinook and coho), run type (for example, spring and fall Chinook salmon), location (for example, tributary population or main-stem reach), or spawner timing (for example, early compared to late).

The dynamics of the S3 model are governed by a series of transition equations, much like stage-structured matrix population models. Transition equations consist of daily survival and movement functions and a growth model that determines when fish grow large enough to transition from one life stage to the next. Within a time step, the order of operations is as follows: First, survival is applied at the beginning of the time step, except in some special cases (for example, when survival depends on distance moved). Surviving fish then grow and possibly transition to the next life stage. Emerging fry and juveniles entering from tributaries are added to the existing abundance in each habitat unit and the mean mass of each life stage is updated. Movement occurs at the end of the time step and mean mass of fish is updated after movement.

Daily survival probability, $S_{p,s}(h, t)$, determines the number of fish surviving from day t to t+1:

$$n^{\mathrm{S}}_{p,a}(h,t) = n_{p,s}(h,t) S_{p,s}(h,t) \tag{1}$$

where the superscript in $n^{\mathrm{S}}_{p,a}(h,t)$ refers to the number remaining in the habitat unit after survival (S) takes place. Note that survival is fully indexed by population, life stage, habitat unit, and time to indicate that user-defined functions allow survival to vary among these population components. For example, $S_{p,s}(h, t)$ may be represented as the product of survival probabilities due to independent causes of mortality such as temperature, density, or size-dependent mortality (see Survival Submodels).

Transition from one juvenile life stage to the next is driven by a growth model that tracks the mean mass of each life stage, $m_{p,s}(h, t)$, by source population and habitat unit. At each time step, the growth model simulates the increase in mean mass using a growth model appropriate for the population under study. When $m_{p,s}(h, t)$ of life stage s exceeds a user-defined maximum size, m^*_s, then fish transition to the next life stage (h and t indexing is omitted here for brevity):

$$n^{\mathrm{SG}}_{p,s+1} = n^{\mathrm{S}}_{p,s} I_{\left(m_{p,s} > m^*_s\right)} + n^{\mathrm{S}}_{p,s+1} \text{ and} \tag{2}$$

$$n^{\mathrm{SG}}_{p,s} = n^{S}_{p,s} \left(1 - I_{\left(m_{p,s} > m^*_s\right)}\right) \tag{3}$$

where the superscript in $n^{\mathrm{SG}}_{p,s+1}$ indicates the number of fish remaining after survival (S) and growth (G) has taken place, s and s+1 represent the current and next life stage, and $I_{\left(m_{p,s} > m^*_s\right)}$ is an indicator function resolving to 1 when $m_{p,s} > m^*_s$. The mass of life stage s+1 is updated as the weighted mean of stage s and s+1 with weights that are proportional to the abundance in each stage. Stage transitions also may be driven by a threshold length (l^*_s), which is then converted to mass using an allometric length-weight relation parameterized for the population of interest.

Next, the number of individuals is updated as new juvenile fish from population p at life stage s enter the model domain as

$$n^{\mathrm{SGE}}_{p,s}(h,t) = n^{\mathrm{SG}}_{p,s}(h,t) + e_{p,s}\left(h,t\right) \tag{4}$$

where $e_{p,s}(h, t)$ is the number of new individuals entering the model domain in habitat unit h at time t, and the superscript in $n^{\mathrm{SGE}}_{p,s}(h,t)$ indicates the number remaining after survival (S), growth (G), and entry (E) of new fish into the habitat unit have occurred. New fish enter the model domain from fry emerging in the main stem and juveniles entering from tributaries or hatcheries. The habitat unit-specific time series of emerging fry arises from an egg survival and development submodel that requires a time series of spawner abundances for each habitat unit as input. For tributary and hatchery juveniles, $e_{p,s}(h, t)$ is specified as a model input.

To implement movement, fish occupying habitat unit *h* are distributed among possible habitat units by assigning the proportion of fish in habitat unit *h* that move to unit *i* in one time step. Across all habitat units, movement proportions form a movement matrix, **M**, with elements $\pi_{i,h}$ representing the probability of moving from habitat unit *h* to habitat unit *i* in one time step. Thus, **M** is an *H* by *H* matrix with columns (indexed by *h*) representing habitat units from which fish move and rows (indexed by *i*) representing the habitat units to which fish may move. Furthermore, the columns of **M** sum to one; that is, $\sum_{i=1}^{H} \pi_{i,h} = 1$ for all *h*.

Over time, movement is implemented as the matrix product of habitat-specific abundance and movement probabilities:

$$\mathbf{n}_{p,s}(t+1) = \mathbf{M}_{p,s}(t)\mathbf{n}_{p,s}^{\mathrm{SGE}}(t) \tag{5}$$

where $\mathbf{n}_{p,s}(t)$ is the vector of habitat unit-specific abundances at time *t* for each source population and life stage, and $\mathbf{n}_{p,s}(t+1)$ is the abundance vector after one time step. Note that $\mathbf{M}_{p,s}(t)$ may be time-specific if movement probabilities are functions of environmental variables or population characteristics such as size or density.

After movement, fish arriving in a given habitat unit at time $t + 1$ comprise individuals that came from many different habitat units at time *t*. Consequently, the mass of fish in unit *i* at time $t+1$ is tracked as the average mass of fish at time *t* weighted by the abundance of fish that came from all *H* habitat units:

$$\mathbf{m}_{p,s}(t+1) = \frac{\mathbf{M}_{p,s}(t)\mathbf{b}_{p,s}(t)}{\mathbf{M}_{p,s}(t)\mathbf{n}_{p,s}(t)} \tag{6}$$

where $\mathbf{b}_{p,s}(t) = \mathbf{n}_{p,s}(t) \circ \mathbf{m}_{p,s}(t)$ is the unit-specific vector of biomass at time *t*, $\circ$ indicates elementwise multiplication, and $\mathbf{m}_{p,s}(t)$ is the vector of mean mass of fish in life stage *s* in each habitat unit at time *t*. In general, any quantitative characteristic of fish that must be tracked after movement uses the form of equation 6.

This modeling framework is quite general and applicable to many alternative species, populations, and life history strategies. In fact, much of the detail that determines how S3 is applied to a particular population lies in specifying functions that determine how survival, growth, and movement respond to environmental, habitat, and density-dependent drivers.

Physical Inputs

Flow and temperature drive many of the population dynamics of juvenile salmonids in S3, either directly (for example, temperature affects growth) or indirectly (for example, flow affects suitable habitat area). Thus, primary inputs to the S3 model are *H* by *T* matrices of water temperature (*Temp*, in degrees Celsius) and discharge (*Q*, in cubic foot per second). The input files follow a flexible format where the user specifies a daily time series of flow and temperature measured at given update locations (river kilometers) along the axis of the river. The S3 model then maps the flow and temperatures to specific habitat units in between update locations by assuming that flow and temperature are constant until the next downstream update location. Additionally, update locations need not be the same for flow and temperature. This allows the user full flexibility in specifying flow and temperature inputs based on the location of available data sources such as streamgages, tributary mouths, or temperature monitoring locations that may not coincide with the location of discharge gaging stations.

For our application of S3 on the Klamath and Trinity Rivers, flow and temperature input files are generated using daily flow and temperature output from the Klamath Basin RBM10 water temperature model (Perry and others, 2011; Risley and others, 2012; Jones and others, 2016). This water temperature model simulates daily mean temperature along the entire river corridor of the Klamath River from Link River Dam to the ocean, and on the Trinity River from the Lewiston Dam to its confluence with the Klamath River.

Habitat Area and Capacity

One of the fundamental concepts of S3 is that daily discharge influences available habitat for different life stages, which in turn drives density-dependent processes that affect population dynamics. Thus, the model requires an *H* by *T* matrix of available habitat areas for each life stage ($A_s(h,t)$, m^2), or an *H* by *T* matrix of habitat capacities ($C_s(h,t)$, number of fish).

The *H* by *T* habitat area or capacity matrix is provided to S3 as input data, which allows the user to choose from a wide array of field and modeling techniques for estimating habitat area or capacity. For the Klamath River, we used habitat suitability criteria (HSC) and weighted usable area (WUA) curves to simulate a daily time series of usable habitat area in each habitat unit. In summary, we first developed HSC curves for depth, velocity, and distance to cover using the methods of Som and others (2015). Next, we applied those curves over a range of flows to the computational cells of eight, two-dimensional (2D) hydrodynamic models for different geomorphic reaches of the Klamath River. WUA curves were then summarized for unique meso-habitat types within the 2D models. The unique habitat units in the 2D models were assigned to unmodeled habitat units of similar habitat structure, and an algorithm was applied to scale all WUA values relative to channel width, length, and differences in discharge. Using this approach, we developed an input data set of $A_s(h,t)$ to drive fish population dynamics. Full details can be found in forthocoming reports for the Klamath River S3 model (Perry, USGS, written oral comm, 2018).

In contrast, on the Trinity River, we simulated both $A_s(h,t)$ and $C_s(h,t)$ directly using statistical models fit to data from an intensive snorkel study, which was then applied to a 2D hydrodynamic model constructed for a 40-mile stretch of the Trinity River. Som and others (2017) developed a statistical model for double-observer snorkel data that was able to estimate (1) the probability of fish presence; (2) the expected mean abundance as a function of depth, velocity, and distance to cover; and(3) temporal and spatial process variation in abundance. We applied this model to the cells of the 2D hydrodynamic model to estimate the probability of presence, and we used the 95th percentile of the predicted abundance distribution as an estimate of capacity. We then summarized over the defined habitat units to obtain estimates of usable area and total capacity. Full details are available in the forthcoming report for the Trinity River (Perry, USGS, written oral comm, 2018).

Many other approaches are possible for developing the spatial structure of habitat units and the habitat input data sets for S3. For example, Hendrix and others (2014) used depth and velocity information from cross sections in HEC-RAS, a one-dimensional steady-state flow model, and combined these data with maximum density estimates to develop habitat capacities in a life cycle model for winter run Chinook salmon in the Sacramento River. Such an approach would work equally well in S3—the HEC-RAS cross sections could be aggregated over logical segments to construct habitat units, and the depth and velocity in each cross section could be used to generate either habitat area or capacity. Additionally, although we give examples for juvenile salmon habitat in this section, similar approaches could be used to construct available spawning habitat, an input that is required to drive the redd superimposition and egg mortality.

Spawning, Egg Development, and Egg Survival Submodel

To simulate the spatiotemporal distribution of emerging fry from natural production occurring within the domain of a model, the S3 model simulates baseline natural mortality of eggs, egg mortality occurring from superimposition and exceedance of thermal maxima, and development of eggs as a function of temperature. The number of fry emerging at time *t* in habitat *h*, $e_{p,\text{fry}}(h,t)$, is:

$$e_{p,\text{fry}}(h,t) = \sum_{i=\min \text{spawn date}}^{\max \text{spawn date}} n_{p,\text{eggs}}(h,i)\, p_{\text{emerge},i}(h,t) \prod_{j=i}^{t} S_{\text{egg}}(h,j) \tag{7}$$

where $n_{p,\text{eggs}}(h,i)$ is the number of eggs deposited on day $t = i$ in habitat unit *h*, $p_{\text{emerge},i}(h,t)$ is the proportion of eggs deposited on day *i* that emerge on day *t*, $\prod_{j=i}^{t} S_{\text{egg}}(h,j)$ is the probability of eggs surviving from spawning day *i* to day *t*, and $S_{\text{egg}}(h,j)$ is the daily survival probability.

Daily egg survival probability is the product of three independent sources of mortality—(1) daily baseline "natural" mortality, (2) temperature-related mortality, and 3) mortality from redd superimposition:

$$S_{\text{egg}}(h,j) = S_{0,\text{egg}} S_{\text{Temp,egg}}(h,j) S_{\text{SI,egg}}(h,j) \tag{8}$$

where $S_{0,\text{egg}}$ is the baseline daily survival probability, $S_{\text{Temp,egg}}(h,j)$ is the daily survival owing to exceedance of thermal tolerance, and $S_{\text{SI,egg}}(h,j)$ is the daily probability of surviving superimposition. Baseline natural mortality is a user-defined daily survival probability that is constant across time and space and determines the proportion of eggs surviving to emergence in the absence of other causes of mortality. Baseline natural mortality was set to $S_{0,\text{egg}} = 0.9975$, which corresponds to a survival probability of 0.687 over a 150-day incubation period. As a basis of comparison, Johnson and others (2012) noted that mean survival of Chinook salmon reared in egg boxes under natural conditions in the Yakima River, Washington, ranged from about 0.6 to 0.85.

Egg survival is known to decrease rapidly at temperatures less than about 4 °C and greater than 15–17 °C (Boles, 1988; Jager, 2011). We used a study by Geist and others (2006), who noted no egg mortality at temperatures less than 17 °C, but high mortality once this threshold was exceeded. Based on this study, we assume that daily egg survival probability was 1 for temperatures less than or equal to 17 °C, yet survival was 0.25 for temperatures greater than 17 °C, resulting in nearly total mortality after 4 days above this threshold temperature (fig. 1). Although survival is known to decrease rapidly at temperatures less than about 4 °C, we do not impose a lower temperature threshold for egg mortality because water temperatures in S3 represent surface-water temperatures, which can differ from intra-gravel water temperatures (David, 2017). Thus, surface temperatures simulated by a temperature model may decrease to less than 4 °C when intra-gravel temperatures remain greater than this temperature.

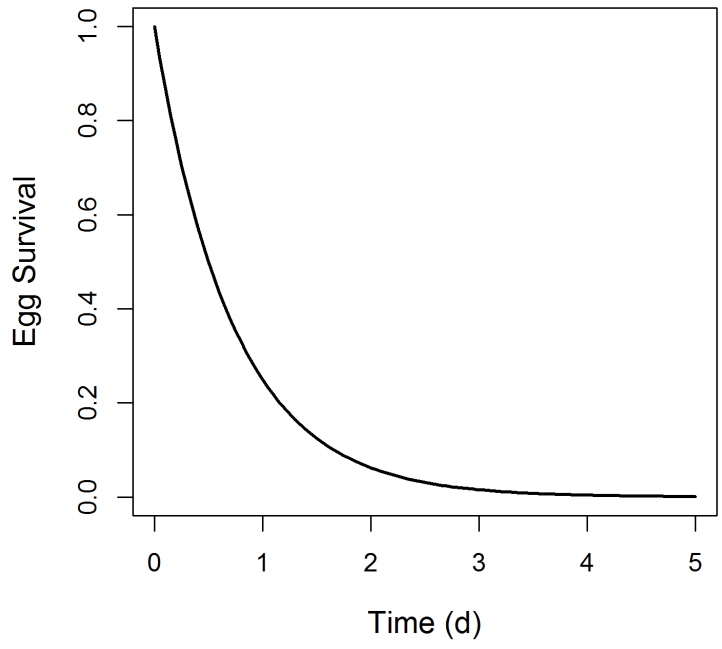

Figure 1. Graph showing total egg survival as a function of time (in days [d]) when water temperature exceeds 17 degrees Celsius.

Although redd scour owing to freshets is known to influence survival of eggs, we have not yet implemented mortality owing to scour in the S3 model. We have investigated several scour functions for the Klamath and Trinity Rivers during the model development phase, but have not included those models because redd scour was not a substantial component of egg mortality in the brood years that we used for calibration. We anticipate that future versions of the S3 model will include an egg scour function.

The number of eggs deposited on a given day ($n_{p,\text{eggs}}(h,i)$) and daily mortality due to superimposition are determined by a simple dynamics model based on the work of Maunder (1997) that uses the daily time series of available spawning habitat to simulate (1) when spawners deposit eggs, and (2) the probability of previously deposited redds being superimposed. If the number of female spawners arriving in habitat unit *h* on day *t* is less than the redd capacity of the habitat unit on day *t*, then all eggs are deposited on day *t*. However, if the number of spawners exceeds capacity, then spawners wait until redd sites become available, at which point all eggs are deposited. The number of eggs deposited is the product of the number of spawners and mean spawner fecundity, a user-defined parameter.

Daily redd capacity, $K(h, t)$, was calculated as:

$$K(h,t) = \frac{A_{\text{spawn}}(h,t)}{A_{\text{redd}}} - g(h,t) \tag{9}$$

where $A_{\text{spawn}}(h,t)$ is the available spawning habitat in unit *h* on day *t* (m^2), A_{redd} is the mean area of each redd, which we set to 4.5 m^2 (Overstreet and others, 2016), and $g(h,t)$ is the number of redds actively guarded in habitat unit *h* on day *t*. The number of guarded redds is determined by a user-defined redd guarding period, which we set to between 7 and 10 days, depending on the application. Finally, $g(h,t)$ is the sum of all spawners that deposit eggs between day *t*-7 and *t*.

The number of redds available for superimposition on day *t* is the total number of redds deposited up to day *t*-1, less the number of actively guarded redds and those redds outside the currently available spawning habitat. Under the simplifying assumption of a random spatial distribution of redds in available spawning habitat, a decline in available spawning habitat from day *t* to *t*+1 implies that some redds will lie outside of the available spawning habitat on day *t*+1. Therefore, when spawning habitat decreases, we calculate the number of redds outside the currently available spawning habitat as the total number of redds multiplied by the proportional decrease in spawning habitat. Given redd capacity, the number of spawners, and the number of redds within the available spawning habitat on day *t*, the daily survival probability owing to superimposition is:

$$S_{\text{SI}}(h,t) = 1 - \left(\frac{n_{\text{spawner}}(h,t)}{K(h,t)} \right) \left(\frac{R_{\text{in}}(h,t)}{R(h,t)} \right) . \tag{10}$$

where all quantities refer to habitat unit *h* on day *t*, $S_{\text{SI}}(h,t)$ is the probability of surviving superimposition, $n_{\text{spawner}}(h,t)$ is the number of spawners depositing eggs, $K(h,t)$ is the redd capacity, $R_{\text{in}}(h,t)$ is the number of previously deposited unguarded redds within the available spawning habitat, and $R(h,t)$ is the total number of previously deposited unguarded redds. The first term represents the probability of superimposition given redds are within the spawning area and not being guarded, and the second term is the proportion of the unguarded redds within the available spawning area on day *t*.

For this model, fig. 2 shows the effect of redd guarding on the relation between the number of female spawners and the number surviving redds as a function of redd guarding duration when available habitat is constant.

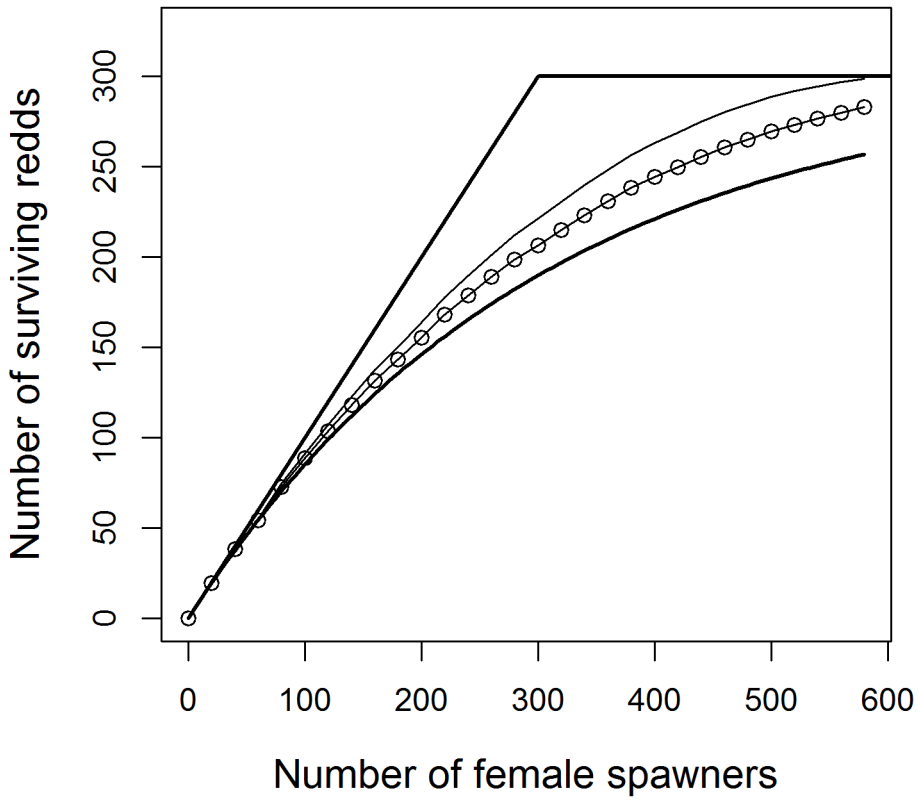

Figure 2. Graph showing effect of red guarding on relation between number of female spawners and number of surviving redds as function of red guarding duration when available habitat is constant (carrying capacity of *K* = 300 redds). Heavy solid lines show the effect of no redd guarding (bottom line) and complete redd guarding (top line). Line with circles shows the effect of a 1-week redd guarding period, and thin line without symbols shows the effect of a 2-week redd guarding period on the number of surviving redds.

Once eggs are deposited, S3 uses an egg development model from Beacham and Murray (1990). We use their "model 2" for Chinook salmon, which models the mean time to emergence as a power function with a minimum temperature threshold (in degrees Celsius) for egg development. Mean time to emergence decreases monotonically with temperature using this model, but degree days to emergence increases with temperature (fig. 3). Because the Beacham and Murray model is based on egg development at constant temperature, we modified it to operate under varying daily temperature by expressing the model in terms of the proportional contribution of each day to full development (fig. 3):

$$P_{\text{dev}}(h,t) = \frac{1}{\exp\left(6.872 - \log(Temp(h,t) + 0.332)\right)} \tag{11}$$

The mean number of days to emergence is determined by satisfying the inequalities:

$$\sum_{i=\text{spawn date}}^{t-1} P_{\text{dev}}(h,i) < 1$$

$$\sum_{i=\text{spawn date}}^{t} P_{\text{dev}}(h,i) > 1 \quad . \tag{12}$$

In short, the mean date of emergence is determined as the first date at which the sum of daily proportional contributions to full development exceeds 1. Additionally, because intra-gravel water temperatures can differ from surface-water temperatures (David, 2017), we provide a user-defined temperature offset that allows users to specify a constant difference between surface and intra-gravel water temperatures.

Although we used the Beacham and Murray (1990) model to determine the mean date of emergence based on accumulation of degree days, emergence times of eggs in a given redd will vary about this mean. Therefore, we assumed that fry emergence follows a normal distribution with the mean degree days to emergence determined by the Beacham and Murray model and the standard deviation in degree days to emergence set to 26.6 days based on data provided in Geist and others (2006). Given this distribution, the probability of emerging on a given date, $p_{\text{emerge},i}(h,t)$ in equation 7, was calculated as the difference in cumulative normal distributions from one day to the next. All fry were assumed to emerge at a mean weight of 0.3 g.

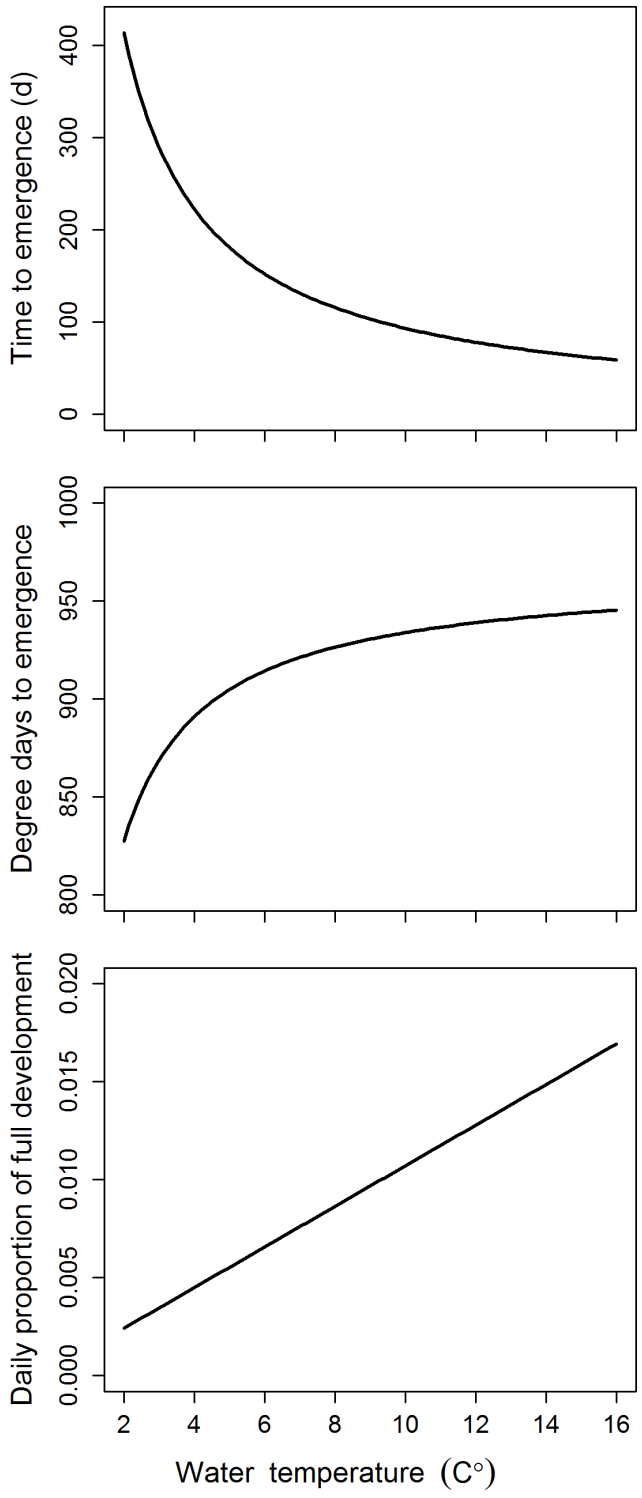

Figure 3. Graph showing Beacham and Murray (1990) egg development model used in Stream Salmonid Simulator (S3) model for Chinook salmon. °C, degrees Celsius; d, days.

Survival Submodels

The riverine environment includes an array of potential mortality causes for juvenile salmonids, some of which are incorporated in S3. For instance, daily survival probability could be the product of baseline survival probability ($S_{0,p,s}(h, t)$), temperature-dependent survival due to exceedance of thermal tolerance, and density-dependent survival. Baseline daily survival is allowed to differ among life stage and source populations, but this structure can be simplified by setting it to the same value across life stages or populations. Density-dependent survival is an optional submodel that may be turned on or off by the user, whereas temperature-dependent survival is implemented in all models (see section, "Density Dependence"). Additionally, other system-specific sources of mortality (for example, predation, disease, water quality) can be included in the S3 framework to simulate daily mortality owing to multiple causes.

In S3, temperature-dependent survival of juvenile Chinook salmon is intended to capture mortality owing to exceedance of physiological thermal tolerance. In contrast, temperature-dependent survival is not intended to include indirect effects of temperature such as the effect of temperature on predation rate or disease. As such, we used data from Brett (1952), who conducted laboratory experiments to quantify the relation between acclimation temperature, water temperature, and time to 50-percent mortality of juvenile Chinook salmon.

To develop the relation between daily survival probability and temperature, we used data from table IV in Brett (1952, p. 316), which recorded the time to 50-percent survival at temperatures ranging from 25 to 27.5 °C. We used data for fish acclimated to 24 °C under the assumption that fish in the wild will have been acclimated to warm water temperatures prior to experiencing temperatures exceeding their thermal tolerance. Brett (1952) noted zero mortality when fish were held for prolonged periods at 24 °C. Therefore, we assumed 100-percent survival at 24 °C. We converted time to 50-percent survival (in minutes) to daily survival by raising 0.5 to t/1,440, where t is time to 50-percent survival and 1,440 is the number of minutes per day (fig. 4). We then fit a logistic regression to the data from table IV, resulting in the following relation:

$$S = \text{ilogit}(57.38 - 2.2*Temp) \quad (13)$$

where ilogit is the inverse logit function (fig. 4).

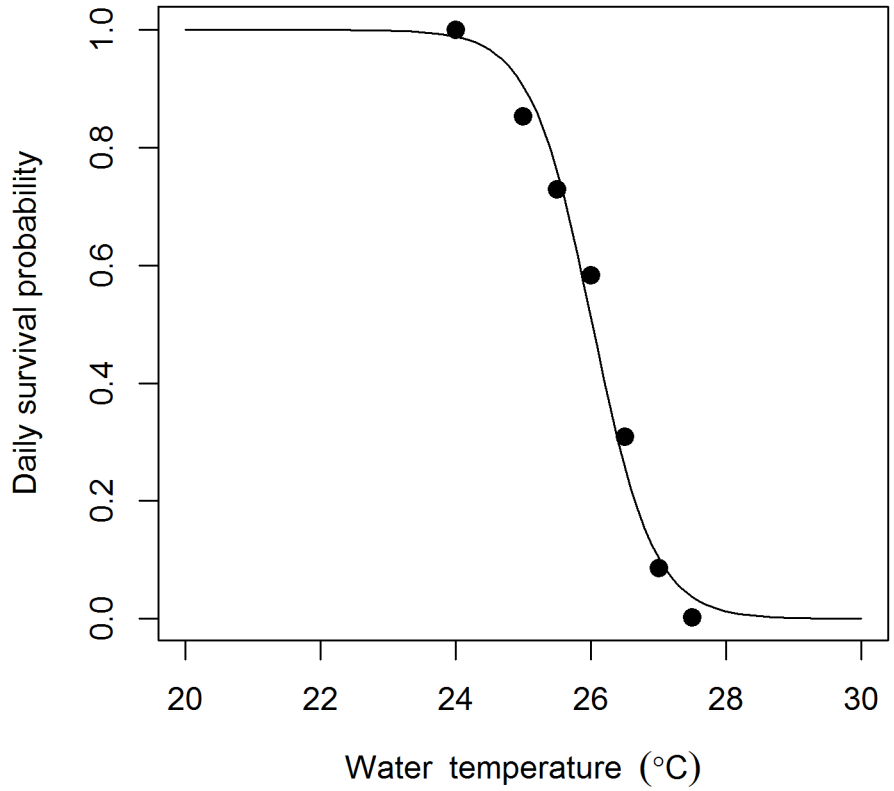

Figure 4. Graph showing fitted relation between water temperature and daily survival probability (black line). Data on the time to 50-percent survival at given temperatures were obtained from Brett (1952) and converted to daily survival probabilities (black circles). °C, degrees Celsius.

Movement Submodels

Although movement probabilities ($\pi_{i,h}$) determine movement dynamics in S3, meaningful biological models for $\pi_{i,h}$ are needed to impart realistic fish movement, to allow movement to respond to abiotic or biotic drivers, and to reduce the number of movement parameters that need to be specified (recall that movement matrix **M** contains H by H movement probabilities). Therefore, we implemented two movement models to represent differences between how rearing fish (for example, fry and parr) move relative to actively migrating fish (for example, smolts). For smolts, we used an advection-diffusion model that was developed for migrating juvenile salmon on the Columbia River (Zabel and Anderson, 1997; Zabel 2002). For fry and parr, we developed the "mover-stayer model"—a two-part model that specifies the probability of fish staying in a given habitat from time t to t+1, and then assigns fish that move a distribution of movement distances.

Advection-Diffusion Model

For smolts, we specified the movement probabilities by integrating a continuous advection-diffusion model across the discrete landscape of habitat units. An advection-diffusion model captures the well-known tendency for a group of fish initially concentrated at a point in space to move downstream (advection) and spread out over time (diffusion; Zabel and Anderson, 1997; Gurarie and others, 2009). This process can be characterized as a traveling, widening wave (fig. 5). One advantage of this model is that movement is determined by two biologically meaningful parameters—the migration rate (r, in kilometers per day) and the diffusion rate (σ^2, in square kilometers per day). Using this model, the spatial distribution of fish originating in habitat unit h after t time steps follows a normal distribution with mean rt and variance $\sigma^2 t$. Here, rt is the average distance moved and $\sigma^2 t$ is the variance of the spatial distribution after t time steps (fig. 5).

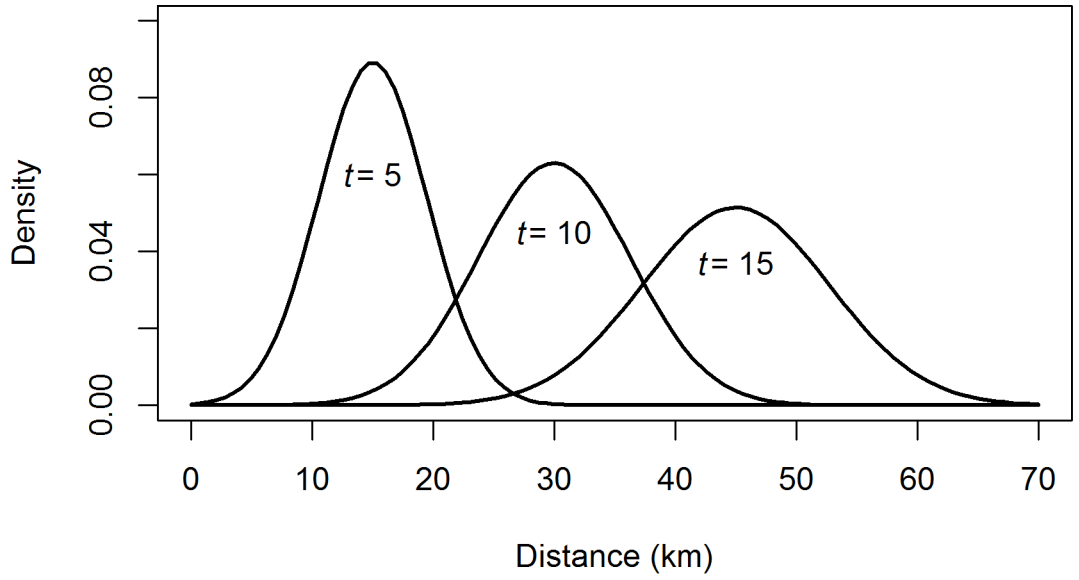

Figure 5. Graph showing spatial distribution of a population after time (t) = 5, 10, and 15 days for a starting point of x = 0, a migration rate of 3 kilometers per day (km/d), and a standard deviation of 2 km/d$^{0.5}$.

For application in S3, movement probabilities from habitat unit h to habitat unit i are calculated by integrating the spatial distribution function between habitat unit boundaries (fig. 2):

$$\pi_{i,h} = \int_{\Delta x_{i,\text{up}}}^{\Delta x_{i,\text{down}}} f\left(x \mid x_h, r, \sigma, \Delta t = 1\right) dx = F\left(\Delta x_{i,\text{down}} \mid x_h, r, \sigma, \Delta t = 1\right) - F\left(\Delta x_{i,\text{up}} \mid x_h, r, \sigma, \Delta t = 1\right) \tag{14}$$

where $\Delta x_{i,\text{up}}$ and $\Delta x_{i,\text{down}}$ are the distance from the midpoint of habitat unit h (x_h) to the upstream and downstream boundaries of habitat unit i, $f(\cdot)$ is the probability density function of the normal distribution, and $F(\cdot)$ is the cumulative distribution function of the normal distribution. In addition to characterizing movement in terms of the mean and variance in migration rate, this approach naturally accounts for habitat units of different length (fig. 6). An example of the application of this movement model within the framework of Klamath River S3 model is shown in figure 7.

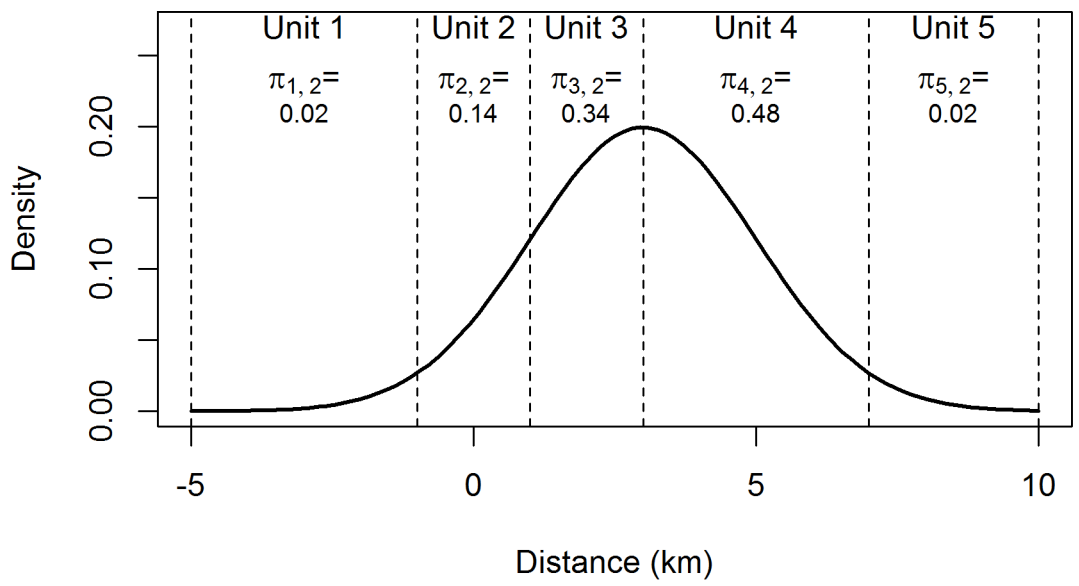

Figure 6. Graph showing example of how the advection-diffusion model is mapped to discrete space to calculate movement probabilities. The solid line shows the spatial distribution of fish originating in habitat unit 2 (x = 0) after migrating for 1 day at a migration rate of 3 kilometers per day (km/d), and a standard deviation of 2 km/d$^{0.5}$. Dashed lines show the location of habitat unit boundaries relative to the midpoint of habitat unit 2. Area under the spatial distribution curve between habitat unit boundaries yields $\pi_{i,h}$, the probability of moving from unit h to unit i in one time step. For example, the probability of moving from unit 2 to unit 4 ($\pi_{4,2}$) is 0.48, whereas the probability of remaining in unit 2 ($\pi_{2,2}$) is 0.14.

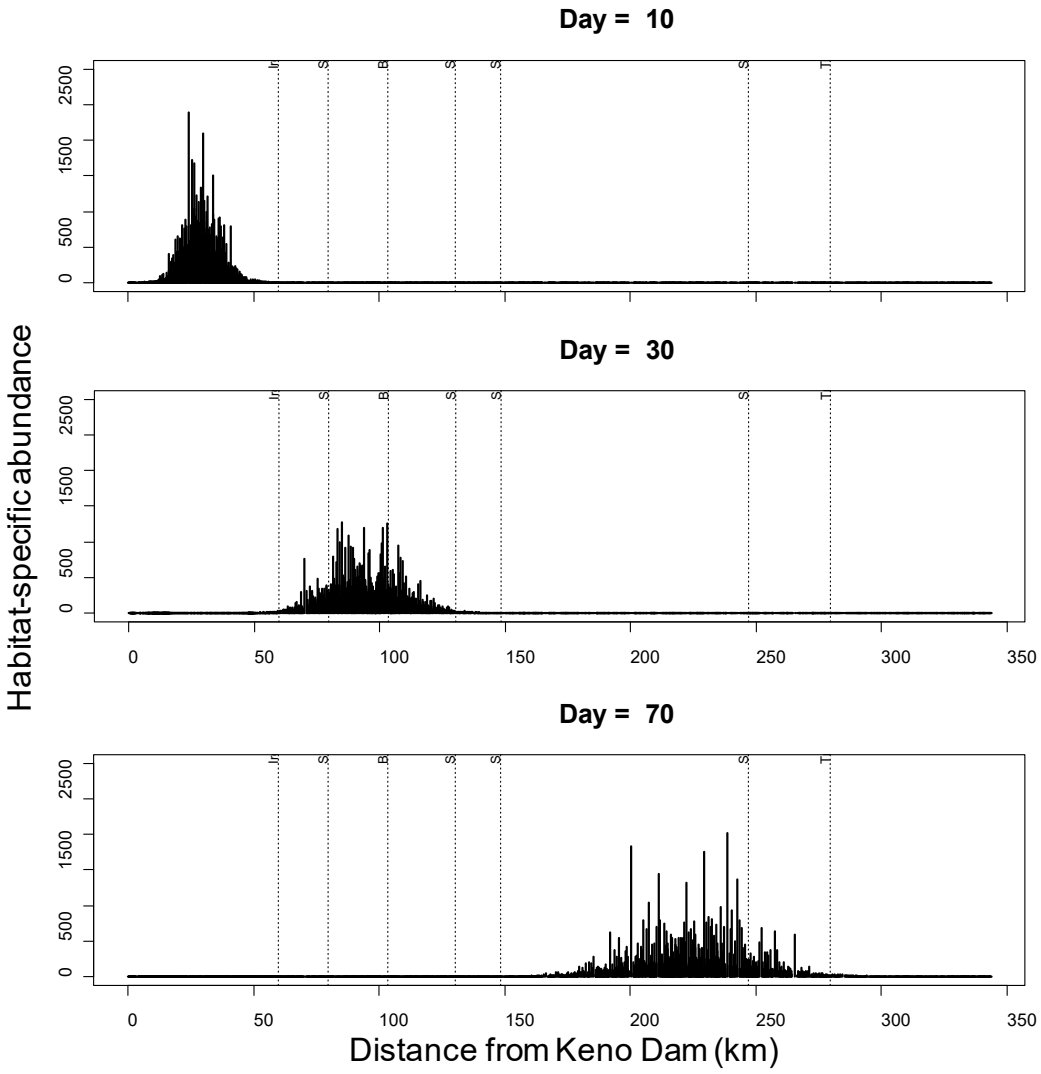

Figure 7. Graphs showing example of the movement model implemented for the Klamath River under a dam removal scenario, with habitat-specific abundance (spatial distribution) after 10 (top graph), 30 (middle graph), and 70 days (bottom graph) for a group of fish "released" at kilometer (km) 0 (Keno Dam) and with a mean migration rate of 3 km per day (km/d) and a standard deviation of 3 km/$d^{0.5}$.

Many different models of movement can be constructed from this general movement framework by allowing r and σ to vary with environmental or individual covariates. For example, Zabel (2002) determined that both r and σ of fall Chinook salmon in the Snake River were positively related to fish size. Other interesting movement relations include density-dependent movement, where r increases with fish density in a given habitat, and flow-related movement, where r increases with river flow or velocity. This movement framework also can be used to simulate the upstream migration of adults. Finally, setting $r = 0$ and $\sigma \geq 0$ simulates a resident non-migratory population that moves among habitats but shows no net population displacement. These examples show how an advection-diffusion model of movement provides a flexible framework for simulating movement of salmon.

In the application of S3 to Klamath and Trinity Rivers, we parameterized the advection-diffusion model using relations developed for fall Chinook salmon on the Columbia River (Zabel, 2002; Plumb, 2012). First, we plotted year-specfic relations between migration rate (r) and fork length reported by Zabel (2002) and Plumb (2012; fig. 8). Next, we visually fit the non-linear relation between migration rate and the cube of fork length:

$$r = 0.095 + \exp\left(-11.3\right) l^3 \tag{15}$$

where l is fork length (fig. 8). An aspect of this relation is that migration rate is approximately linear and equal in magnitude to the weight of a fish in grams. Furthermore, although we developed this model for all fish sizes, we applied it only to actively migrating smolts, which is determined by the user-defined size cutoff for the parr-smolt transition. Next, we assumed a constant value of 21.1 $km/d^{0.5}$ for σ based on the mean estimated values of σ reported by Zabel (2002) and Plumb (2012).

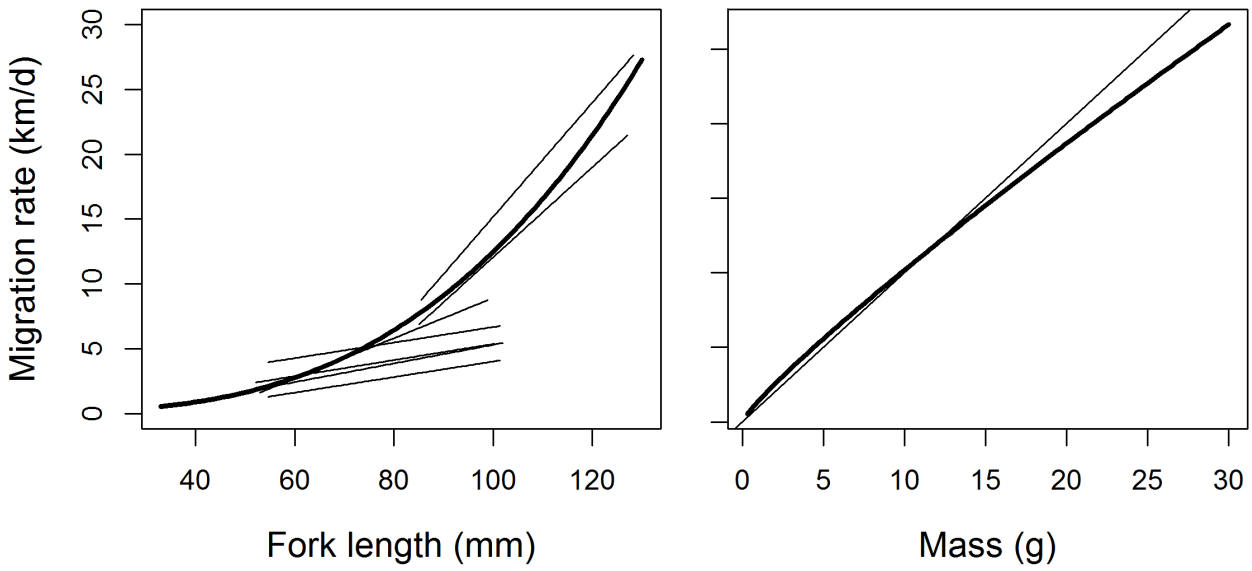

Figure 8. Graphs showing estimated relations between migration rate (in kilometers per day [km/d]) and fork length (in millimeters [mm]) from Zabel (2002) and Plumb (2012) (left graph), and between migration rate and fish mass (in grams [g]) (right graph). Thin lines represent the relation from Zabel (2002) and Plumb (2012, and heavy lines represent the relation used in the Stream Salmonid Simulator (S3) model. In the right graph, the thin diagonal line shows where the migration rate is equal to fish mass.

Mover-Stayer Model

The mover-stayer model is intended to capture the tendency for most fry and parr to remain in a given habitat during rearing while allowing some small fraction to disperse downstream. The mover-stayer model has two parameters:— $P_{\text{stay}}(h,t)$, the probability of fish staying in habitat unit h between time t and t+1; and $\mu_{\text{move}}(h,t)$, the mean distance moved downstream for fish that leave habitat unit h between time t and t+1. For movers, we assumed that the movement distance follows an exponential distribution with mean distance $\mu_{\text{move}}(h,t)$, which can either be expressed as a constant or a function of the mean fish length (fig. 8). We then used an approach similar to that of the advection-diffusion model to map the continuous distribution of movement distance to the discrete habitat structure of S3. To determine movement probabilities in $\mathbf{M}_{p,s}$, we calculated the probability of moving to habitat unit i, conditional on moving out of habitat unit h:

$$\begin{aligned}
&\pi_{i,h} = P_{\text{stay}}\left(h,t\right) \text{ for } i = h,\\
&\pi_{i,h} = \left(1 - P_{\text{stay}}\left(h,t\right)\right)\left[G\left(\Delta x_{i,\text{down}} \mid x_h, \mu_{\text{move}}\right) - G\left(\Delta x_{i,\text{up}} \mid x_h, \mu_{\text{move}}\right)\right] \text{ for } i < h \text{ (i.e., downstream of } h),\\
&\pi_{i,h} = 0 \text{ for } i > h \text{ (i.e., upstream of } h)
\end{aligned} \tag{16}$$

where $\Delta x_{i,\text{up}}$ and $\Delta x_{i,\text{down}}$ are the distance from the midpoint of habitat unit h (x_h) to the upstream and downstream boundaries of habitat unit i, and $G(\cdot)$ is the cumulative distribution function of the exponential distribution.

Growth Submodels

The S3 model provides the user with two options for simulating fish growth for juvenile Chinook salmon—(1) A simple 5-parameter model that simulates growth as a function of fish size and temperature (the "Ratkowski" model; Perry and others, 2015), or (2) a 20-parameter model that also includes food consumption (the Wisconsin bioenergetics model; Stewart and Ibarra, 1991).

The Ratkowski Growth Model

The Ratkowski growth model was calibrated to data from 11 studies and 9 watersheds of subyearling Chinook salmon (including the Klamath River) that were fed an *ad libidum* ration in a laboratory or hatchery setting. The model requires daily water temperatures, an initial weight, and a set of temperature- and mass-dependent parameters (Perry and others, 2015; table 1) to calculate average fish mass on day t + 1 from fish mass on day t for fish in habitat unit h. The growth rates produced by the Ratkowski model represent the growth rates of fish fed an at *ad libidum* ration. In our application, the growth rates of juvenile Chinook salmon produced by the Ratkowski model are similar to growth rates produced at two-thirds of maximum consumption in the Wisconsin bioenergetics model (fig. 9).

The Perry and others (2015) version of the Ratkowski model expresses mass-standardized growth rates as a function of temperature:

$$\Omega = d\left(T - T_{\mathrm{L}}\right)\left(1 - e^{g\left(T - T_{\mathrm{U}}\right)}\right) \text{ or} \tag{17}$$

$$\Omega = d\left(T - T_{\mathrm{L}}\right)\left(1 - e^{g\left(T - T_{\mathrm{M}}\right)}\left(1 + g\left(T_{\mathrm{M}} - T_{\mathrm{L}}\right)\right)\right) \tag{18}$$

where Ω is the mass-standardized growth rate expressed as the growth rate (in percent of a 1-g fish, d and g are shape parameters, T_{L} and T_{U} are the lower and upper temperature limits where growth rate is zero, and T_{M} is the optimal temperature at which growth is maximized.

Mass at time t+1, M_{t+1}, is calculated from mass at time t as:

$$M_{t+1} = \left(M_t^b + \frac{\Omega b}{100}\right)^{\frac{1}{b}} \tag{19}$$

where b is the allometric mass exponent. Initial fish mass at the time of emergence was set 0.3 g.

Table 1. Estimates of mass- and temperature-dependent growth parameters of juvenile Chinook salmon obtained from fitting the Ratkowski model to growth data from 11 studies in 9 watersheds.

[b is the allometric growth exponent, d and g are shape parameters of the Ratkowsky model, T_{L} is the lower temperature limit for growth, T_{M} is the temperature at which growth is maximized, T_{U} is the upper temperature limit for growth, c is the specific growth rate of a 1-gram fish at T_{M}, and σ is the residual standard deviation of the model fit to the data (see Perry and others, 2015)]

Parameter	Estimate	Standard error	95-percent confidence interval
b	0.338	0.025	0.290, 0.386
d	0.415	0.037	0.342, 0.488
g	0.315	0.044	0.228, 0.402
T_{L}	1.833	0.631	0.597, 3.070
T_{M}	19.019	0.271	18.489, 19.550
T_{U}	24.918	0.020	24.878, 24.958
c	6.016	0.059	5.901, 6.131
σ	0.097	0.005	0.087, 0.107

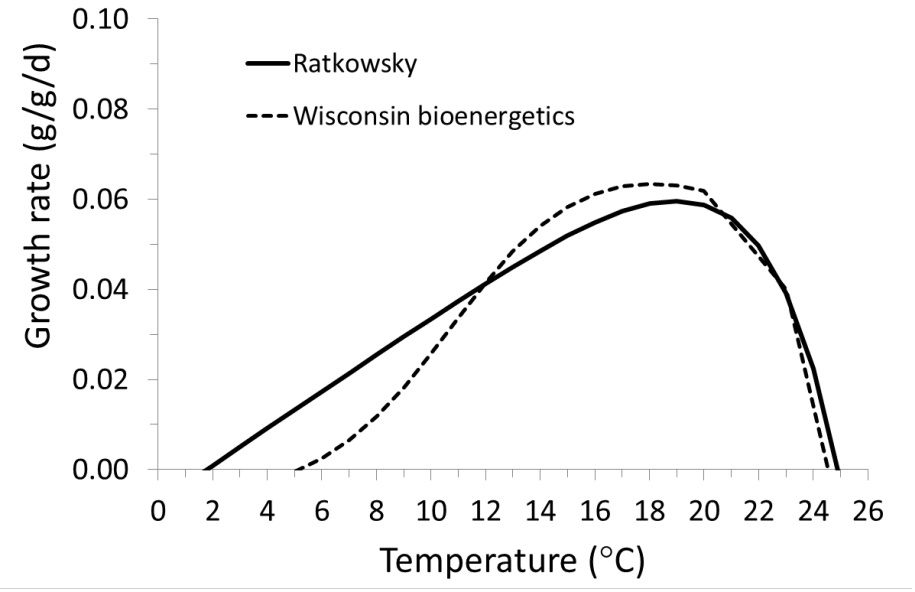

Figure 9. Graph showing comparison of growth rate of a 1-gram Chinook salmon under the Ratkowsky and the Wisconsin Bioenergetics models, where the proportion of maximum consumption was set to 0.66. °C, degrees Celsius; g/g/d, gram per gram per day.

The Wisconsin Bioenergetics Model

The second option for predicting growth in S3 is the "Wisconsin" bioenergetics model for Chinook salmon (Stewart and Ibarra, 1991; Plumb and Moffitt, 2015). Bioenergetics models are a series of log-linear regression equations that have been calibrated from laboratory studies (Stewart and others, 1983; Hanson and others, 1997). These equations predict the metabolic costs and benefits associated with physiological processes such as respiration (*R*), consumption (*C*), specific dynamic action (*SDA*), egestion (*F*), and excretion (*U*), which are dictated by allometric and temperature-dependent functions that require information on the initial fish size and the temperatures occupied at discrete time steps over a specified time horizon. The metabolic costs are reconciled with the amount of food that is consumed in a mass-balance framework

$$M_{t+1} = M_t + C_t - \left(SDA_t + R_t + U_t + F_t\right) \tag{20}$$

where *SDA*, *R*, *U*, and *F* represent daily metabolic costs that are estimated from the log-linear regression equations that were calibrated during laboratory evaluations and assembled by Stewart and Ibarra (1991; table 2). These costs are subtracted from the energetic benefits of food consumed (*C*) on day *t*.

Juvenile fall Chinook salmon have been shown to have higher consumption at warmer water temperatures than that expected from the formulation of the bioenergetics model for Chinook salmon because this formulation uses a consumption function based on Coho salmon. However, Plumb and Moffitt (2015) showed that maximum consumption for juvenile Chinook salmon occurred at a higher temperature than for coho salmon. Therefore, we modified the Stewart and Ibarra (1991) formulation of the model to use the consumption parameters for temperature-dependence in maximum consumption reported by Plumb and Moffitt (2015).

The difference between daily consumption (benefit) and metabolism (costs) is added to the fish weight on the current time step to obtain the average weight of fish at the next time step. Accordingly, the required input for the bioenergetics model for each habitat unit *i* is:

1. Daily water temperatures (°C),
2. Diet composition (we assumed a diet of aquatic invertebrates with 22-percent indigestible matter),
3. Prey energy density (we assumed prey energy density was equal to the fish energy density, and
4. Fish energy density (*Q*; table 2).

When implemented in S3, we assumed a constant consumption rate equal to two-thirds of the maximum possible consumption. Other alternative model structures allow the proportion of maximum consumption to vary with fish density (see section, "Density Dependence").

Table 2. Symbols, parameter descriptions, and nomimal values from the unadjusted Stewart and Ibarra (1991) bioenergetics model for coho and Chinook salmon.

[Symbols are those reported by Hanson and others (1997). Temperature-dependent consumption parameters were obtained from Plumb and Moffitt (2015). The parameter values for $K_{1\text{-}4}$ used in the adjusted bioenergetics model are also shown. The letter *W* represents fish body weight (in grams) and *T* represents water temperature (in degrees Celsius)]

Symbol	Parameter description	Equation or nominal value
Q	Weight-dependent energy density for fish less than 4 kilograms	=5763+0.986·W
	Maximum consumption, C_{max}	
CA	Intercept: C_{max} at $(K_2+K_3)/2$	0.303
CB	C_{max} vs. Weight	-0.275
CQ	Temperature for K_1	4.97
CTO	Temperature for K_2	20.93
CTM	Temperature for K_3	20.93
CTL	Temperature for K_4	24.05
*CK*1	Proportion of C_{max} at *CQ*	0.09
*CK*4	Proportion of C_{max} at *CTL*	0.53
P	Proportion of C_{max}	Assumed equal to 0.66
	Respiration, *R*	
RA	Intercept:	0.00264 (grams O_2 per day)
RB	Coefficient: *R* compared to *W*	-0.217
RQ	Coefficient: *R* compared to *T*	0.06818
SDA	Specific dynamic action	0.172
	Egestion, *F*	
FA	Intercept	0.212
FB	Coefficient: *T* compared to egestion	-0.222
FG	Coefficient: *P* compared to egestion	0.631
	Excretion, *E*	
UA	Intercept	0.0314
UB	Coefficient: *T* compared to egestion	0.58
UG	Coefficient: *P* compared to egestion	-0.299

Density Dependence

We link habitat area or capacity to density-dependent population dynamics using a multi-stage Beverton-Holt model (Moussalli and Hilborn, 1986). The Beverton-Holt model is a useful general model because it can be derived from theory regarding foraging, predation risk, and territorial behavior typical of juvenile salmonids (Walters and Korman, 1999). We implemented the Beverton-Holt model as follows:

$$\theta_s(h,t) = \frac{1}{\frac{1}{\theta_0} + \frac{n_{.,s}(h,t)}{C_s(h,t)}} \tag{21}$$

where θ_s is a probability on the (0, 1) scale that may be used to drive survival, movement, or growth; $n_{.,s}(h,t)$ is the total number of individuals of life stage *s* in habitat unit *h* at time *t* (the "." indicates summation over source populations); θ_0 is the intercept and also is known as the productivity parameter; and $C_s(h,t)$ is the total capacity (number of fish) for life stage *s* in habitat unit *h* at time *t*. The Beverton-Holt model produces a monotonically declining curve of θ_s (that is, declining survival, P_{stay}, or growth rate) as the ratio of abundance to capacity increases (that is, increasing density).

In our application of the S3 model, we have implemented alternative model structures where $\theta_s(h,t)$ represents either a daily survival probability, the probability of remaining in a habitat unit in the mover-stayer model (P_{stay}), or the proportion of maximum consumption in the Wisconsin bioenergetics model. S3 provides the flexibility to allow all, none, or different combinations of survival, growth, and movement processes to be density dependent.

The total capacity also may be expressed as a function of the available habitat area and per-unit-area capacity:

$$C_s(h,t) = c_s A_s(h,t) \tag{22}$$

where c_s is the capacity expressed as a maximum density (in number per square meter) and $A_s(h,t)$ is the habitat area (in square meters). If only habitat area is provided as an input, the model has two parameters, θ_0 and c_s. If capacity is provided $C_s(h,t)$ as input, then the model has a single parameter, θ_0. Our application of S3 on the Klamath and Trinity Rivers has used both approaches.

Model Summary and Output

Parameterization of the S3 model is very flexible, depending on whether a particular submodel is "turned on" and whether parameters are set to differ by life stage or source population (fig. 10, table 3). For example, for the Klamath River, we developed a disease submodel to simulate effects of *C. shasta* on infection and mortality of juvenile Chinook salmon, but this submodel is not applied to the Trinity River. As another example, although we developed submodels for density-dependent growth, survival, and movement, we compared the fit of alternative models to data where each model implements only one density-dependent process at a time. Given the flexibility of the model, the number of unique parameters that drive the model will vary. For instance, the S3 model has 19 parameters (excluding the growth and disease models) for the simplest model structure with constant survival and movement rates (table 3). Growth models add another 5 or 20 parameters, depending on choice of growth submodel. Selecting density-dependent submodels and allowing parameters of submodels to vary across life stages increase the number of parameters in the model.

The essential output of the model is H by T matrices containing the daily number of fish and the mean size for each life stage and subpopulation. Additionally, H by T matrices of survival probabilities and movement parameters (for example, P_{move}) provide insights into the spatiotemporal dynamics driving survival and movement. Abundance and size can be plotted over time for a given habitat unit, over space for a given point in time, or animated over time. Abundance and size matrices also can be summarized by summing over life stage and population source.The S3 model deterministically simulates population dynamics; that is, given a fixed set of physical and biological inputs, the model will return exactly the same H x T output matrices even if run multiple times. A future version of the S3 model will allow model runs under a Monte-Carlo framework to propagate constrained parameter uncertainty into model outputs.

Although these matrices fully describe the spatial and temporal changes in abundance and size, monitoring programs often quantify juvenile fish production by estimating the abundance and size of juvenile fish passing a given location in the river (for example, using a rotary screw trap). The S3 model simulates the number of fish in each habitat unit on each day, not the number of fish moving past a given habitat unit each day. Nonetheless, the movement probability matrix (**M)** provides the required information to calculate the flux of fish moving past a given habitat each day. If $n_{p,s}(h,t)$ is the number if fish occupying habitat unit h on day t, then let $n_{p,s}(h^*,t)$ represent the number of fish moving past some habitat unit of interest, h^*, on day t:

$$n_{p,s}(h^*,t) = \sum_{h \le h^*} \left[n_{p,s}^{\text{SG}}(h,t) \sum_{i > h^*} \pi_{i,h} \right] . \tag{23}$$

The first summation inside the brackets sums the probabilities of moving from habitat unit h to all habitat units downstream of h^*; that is, the total probability of moving from unit h past unit h^*. Multiplying this term by the number of fish in habitat unit h (after survival and growth have occurred) yields that number of fish passing unit h^* from habitat unit h. The last summation term calculates the total number of fish moving past unit h^* by summing the number of fish moving past unit h^* from all habitat units upstream of h^*.

The biomass of fish moving past unit h^* for each life stage and source population is calculated similarly:

$$b_{p,s}(h^*,t) = \sum_{h \le h^*} \left[m_{p,s}(h,t)\, n_{p,s}^{\mathrm{SG}}(h,t) \sum_{i>h^*} \pi_{i,h} \right], \tag{24}$$

and the mean size of fish moving past unit h, $m_{p,s}(h^*,t)$ is simply $b_{p,s}(h^*,t) / n_{p,s}(h^*,t)$.

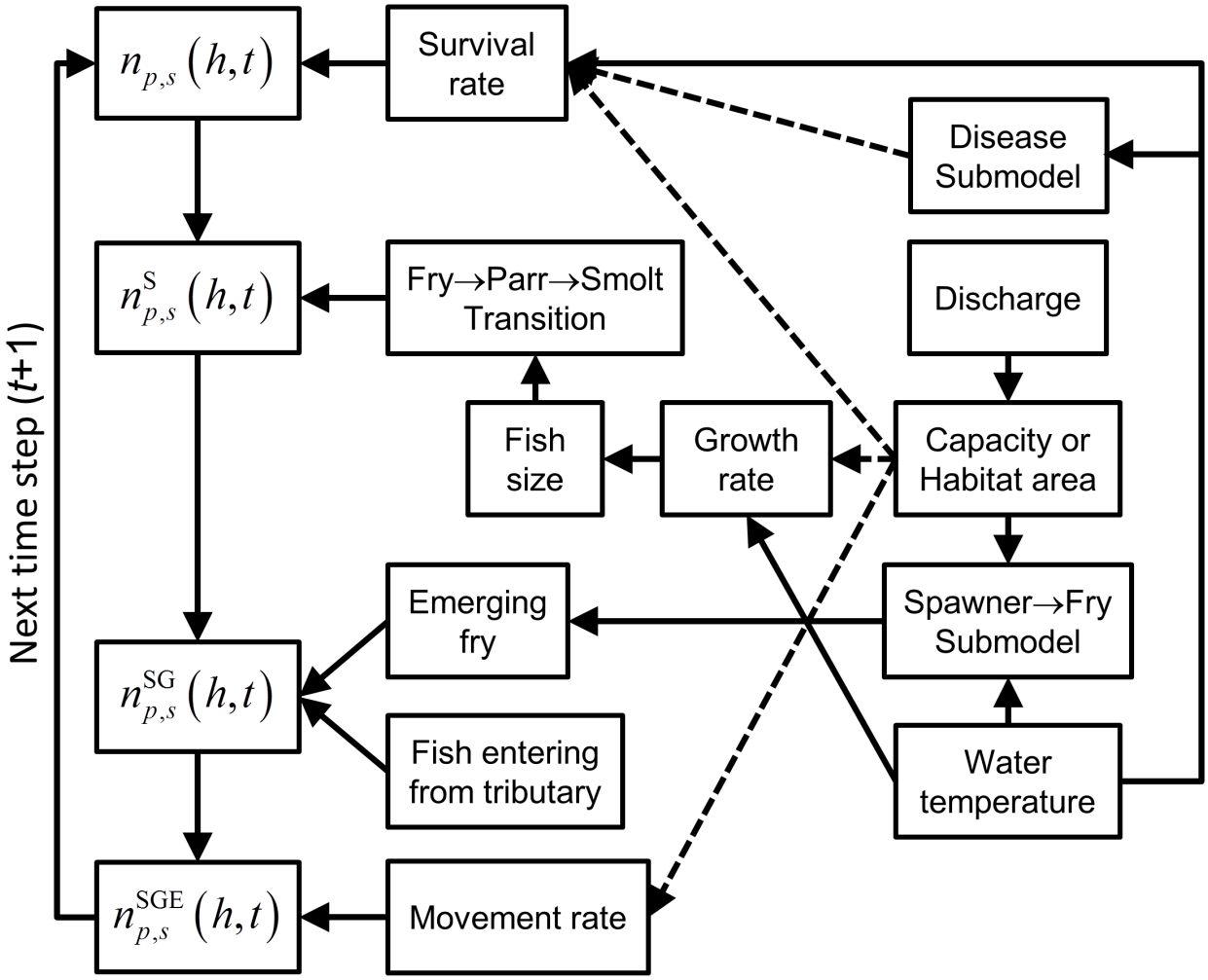

Figure 10. Schematic summary of the Stream Salmonid Simulator (S3) model showing linkages between physical drivers, demographic processes, and changes in daily abundance. Dashed lines show submodels that that may be turned on or off to represent different dynamic processes in the S3 model.

Table 3. Description of parameters and submodels used in Stream Salmonid Simulator (S3) model.

[**Number of parameters:** *P*, number of source populations modeled. **Parameter source:** U, user defined; L, literature; E, estimated through calibration. **Abbreviation:** WUA, weighted usable area]

Parameter or submodel	Description	Number of parameters	Parameter source	Comments
m^*	Maximum size of life stage	2	U	
$S_{0,egg}$	Baseline daily egg mortality	1	U	
$S_{Temp,egg}$	Egg survival as a function of temperature	2	L	
Superimposition	Redd area, mean fecundity, redd guarding period	3	L, U	
Egg development	Intercept and slope for mean emergence date, standard deviation in emergence date, size at emergence	4	L	Function of degree days.
Juvenile survival constant rate	Baseline daily mortality rate	1 to 3*P	U, E	Can set by life stage and source population.
Density dependent survival based on WUA	S_0 and maximum density	2 to 2*3*P	U, E	Can set by life stage and source population.
Temperature-dependent survival	Intercept and slope	2	U, L	
Density dependent survival based on capacity	Capacity given, requires only S_0	1 to 3*P	U, E	Can set by life stage and source population
Advection-diffusion model	Migration rate and diffusion rate	3	L	Applied to smolts only. Migration rate is function of fork length.
Mover-stayer model	P_{stay} and μ_{move}	2 to 2*2*P	U, E	Applied to fry and parr only. Parameters can be set separately by life stage and source population.
Density -dependent mover-stayer model	P_{stay} function of density	2 to 2*2*P	U, E	Applied to fry and parr only. Parameters can be set separately by life stage and source population. If only WUA and not capacity is available, an additional parameter is required (maximum density).
Ratkowsky growth model	Function of temperature and fish size	5	L	
Wisconsin bioenergetics model	Function of temperature, fish size, and ration	20	L	
Density-dependent growth	Beverton-Holt function for proportion of maximum consumption or proportion of growth increment.	1 to 3*P	U, E	Parameters can be set separately by life stage and source population. If only WUA and not capacity is available, an additional parameter is required (maximum density).
Disease submodel (see Perry and others, 2018a in review)	Infection and mortality given infection	9	L	

The summary metrics $m_{p,s}(h^*,t)$, $b_{p,s}(h^*,t)$ and $n_{p,s}(h^*,t)$ fully summarize daily juvenile production upstream of unit *h**. These metrics can be aggregated over weekly time periods, life stages, and source populations for direct comparison to observed abundance estimates from trapping efforts. For example, we calibrated S3 for the Klamath and Trinity Rivers by aggregating daily simulated abundance moving past trapping sites over weekly time periods and fitting the model to observed weekly abundance estimates from long-term monitoring programs. These summary metrics also may be aggregated over a migration year to estimate total annual production that occurs upstream of any habitat unit of interest, *h**. From annual production estimates, total annual survival may be calculated as the abundance emigrating past unit *h** divided by the total number of emerging fry and juveniles entering from tributaries upstream of unit *h**. Overall, there is much flexibility in the ways in which S3 output can be summarized.

Discussion

We developed the S3 model to help resource managers evaluate the effect of management alternatives on juvenile salmonid populations. The general S3 model structure provides a biological and physical framework for the salmonid freshwater life cycle. This framework is targeted to capture important demographics of juvenile salmonids and to translate management alternatives into simulated population responses. Although the S3 model is built on this common framework, the model also has been constructed to allow much flexibility for applications of the model to specific river systems. The ability for practitioners to include system-specific information for the survival, growth, and movement processes ensures that simulations provide results that are relevant to the questions asked and population under study.

Although numerous salmonid life cycle models are available for modeling the effect of management actions in freshwater on salmon populations, few detailed models have been designed to:

1. Be generally applicable to multiple watersheds,
2. Explicitly incorporate all three key demographic processes that affect population dynamics of juvenile salmonids in freshwater (growth, movement, and survival),
3. Include detailed spatial structure at the level of meso-habitat units, and
4. Be able to run on temporal and spatial scales to evaluate a range of management actions typically encountered in management of regulated rivers (for example, water temperature, river flows, and habitat restoration).

Other models capture some of these elements but have been designed for either broader (entire watersheds) or narrower (short stream reaches) applications. For example, the Shiraz model is a general modeling framework for quantifying the effect of habitat management actions on salmon populations at the landscape scale (Scheuerell and others, 2006). Like S3, this model is general enough to be applied to multiple watersheds, uses a multistage Beverton-Holt model to link survival to habitat capacity, and incorporates fish movement. In contrast to S3, the Shiraz model runs on annual time step, does not include fish growth, simulates the entire life cycle, and is designed for modeling an entire watershed and its network of channels. At the opposite end of the spectrum of spatial scale and extent, inSALMO is a detailed individual based model (IBM) designed to simulate effects of river management actions on freshwater life stages of anadromous salmonids (Railsback and others, 2013). Like S3, inSALMO simulates growth, movement, and survival on a daily timescale and is focused only on freshwater life stages. In contrast to S3, inSALMO is stochastic, simulates individuals, represents the stream in two dimensions as a series of contiguous cells, and explicitly models effects of food availability and consumption on growth.

Population models for anadromous salmonids are tailored to answer specific types of management questions by tailoring model dynamics to be sensitive to management alternatives and structuring model output to include key biological metrics. For example, the Shiraz model is designed for evaluating broad-scale management actions at the sub-basin level. In contrast, inSALMO is designed for evaluating fine-scale actions at the reach level such as comparing restored and degraded sites (Railsback and others, 2013). On the spectrum of model complexity, S3 lies between Shiraz and inSALMO, attempting to strike a balance between a spatial extent and biological, temporal, and spatial resolution. The S3 model has the ability to model an entire main-stem river but retains finer-level detail such as tracking daily growth, survival, and movement at the meso-habitat scale. These qualities make S3 well designed for evaluating both broad-scale management actions (such as alternative habitat restoration strategies) and detailed management strategies such as daily flow and temperature management in rivers regulated by dams. In comparison, although inSALMO simulates very detailed individual dynamics in two dimensions, its application likely is limited to short reaches owing to the computational burden of extending to an entire river. Likewise, although Shiraz can simulate an entire main-stem river and its tributaries, its coarse temporal and spatial scale limits its application for understanding more detailed management actions and population responses typical of regulated rivers (for example, evaluating the effect of daily hydrographs).

The examples provided in this report highlight another benefit of the plug-and-play S3 submodel construction in context of population dynamics simulation models—the balance between data-informed and literature-informed demographic parameter values. Those wishing to apply the S3 model to their system are not required to directly estimate all survival, growth, and movement parameters. For aspects of the S3 framework for which localized information is not available, initial applications can begin with literature-derived parameters, or information borrowed from nearby or similarly structured systems. As new and updated information becomes available—for instance through an adaptive management framework or through targeted scientific experiments—submodels can be quickly constructed and "plugged-in" for refined model calibration or simulation runs.

As with balancing the extent and resolution of the S3 model, choice of software platform for implementing the model must strike a balance among aspects of implementation such as model run time, graphical capabilities, built-in statistical procedures, open-source sharing, and ability to support a user interface. For example, coding the model in native languages such as C++ or Fortran may yield the quickest-running model, but such languages have the fewest built-in support features such as graphical packages. Therefore, we have chosen to code the model in the R statistical modeling platform (R Core Team, 2015). The strength of R is its rich library of built-in graphical and statistical packages for building the model and visualizing model output. Furthermore, R is an open-source software package, freely available for anyone to use. Recent additions to the R family include Shiny, an R package for building interactive web applications through R (https://shiny.rstudio.com/). Although R is not the most computationally efficient programming language for running S3 simulations, these benefits far outweigh the run time costs. In the future, we plan to develop S3 in a distributable R package that includes a user interface and model dashboard built in Shiny. Such an interface would allow a user to run the model for a given set of inputs, vary parameters (for example, daily survival rate of eggs), visualize and animate the output, and export model output for further analysis.

The S3 model is a scientifically and computationally mature salmonid population dynamics model. The submodel structure and overall framework show great promise as a tool for helping resource managers evaluate the potential impacts of management alternatives to salmonid populations. Although this report focuses on the overall model structure and submodel examples, companion documents with applications to the Klamath and Trinity Rivers describe submodel characteristics in much greater detail. We look forward to future applications of the Stream Salmonid Simulator as a decision-making tool for resource managers.

Acknowledgments

This work was supported by an interagency agreement #4500054074 with the U.S. Fish and Wildlife Service. We are grateful to Sam Williamson and Tom Shaw for many engaging discussions about how to model juvenile salmon and the factors that influence juvenile salmon population dynamics on the Klamath and Trinity Rivers. This project would not have been possible without the engagement and collaboration among many federal, state, and tribal entities that contributed data with which to construct the S3 model. We thank Jonny Armostrong and Noble Hendrix for providing comments that improved the manuscript.

References Cited

Bartholow, J., Heasley, J., Laake, J., Sandelin, J., Coughlan, B.A.K., and Moos, A., 2002, SALMOD—A population model for salmonids—User's manual, version W3: Fort Collins, Colorado, U.S. Geological Survey, 76 p., accessed November 29, 2017, at citeseerx.ist.psu.edu/viewdoc/download?doi=10.1.1.386.2594&rep=rep1&type=pdf.

Bartholow, J.M., 1996, Sensitivity of a salmon population model to alternative formulations and initial conditions: Ecological Modelling, v. 88, nos. 1–3, p. 215–226.

Bartholow, J.M., Laake, J.L., Stalnaker, C.B., and Williamson, S.C., 1993, A salmonid population model with emphasis on habitat limitations: Rivers, v. 4, no. 4, p. 265–279.

Beacham, T.D., and Murray, C.B., 1990. Temperature, egg size, and development of embryos and alevins of five species of Pacific salmon—A comparative analysis: Transactions of the American Fisheries Society, v. 119, no. 6, p. 927–945.

Boles, G.L., Water temperature effects on Chinook salmon (*Oncorhynchus tshawytscha*) with emphasis on the Sacramento River, 1988: Sacramento, California Department of Water Resources, 48 p.

Brett, J.R., 1952, Temperature tolerance in young Pacific salmon, genus *Oncorhynchus*: Journal of the Fisheries Research Board of Canada, v. 9, p. 265–323.

David, A.T., 2017, Klamath and Trinity River intra-gravel water temperatures, 2015 and 2016: Arcata, California, U.S. Fish and Wildlife Service, Arcata Fish and Wildlife Office, Arcata Fisheries Data Series Report Number DS 2017-49, 23 p.

Geist, D.R., Abernethy, C.S., Hand, K.D., Cullinan, V.I., Chandler, J.A., and Groves, P.A., 2006, Survival, development, and growth of fall Chinook salmon embryos, alevins, and fry exposed to variable thermal and dissolved oxygen regimes: Transactions of the American Fisheries Society, v, 135, no. 6, p. 1,462–1,477.

Gurarie, E., Anderson, J.J., and Zabel, R.W., 2009, Continuous models of population-level heterogeneity inform analysis of animal dispersal and migration: Ecology, v. 90, p. 2,233–2,242.

Hanson, P.C., Johnson, T.B., Schindler, D.E., and Kitchell, J.F., 1997, Fish bioenergetics 3.0: Madison, University of Wisconsin, Sea Grant Institute, WISCU-T-97-001.

Hardy, T.B., Addley, R.C., and Saraeva, E., 2006, Evaluation of instream flow needs in the lower Klamath River—Phase II final report: Prepared for the U.S. Department of Interior by the Institute for Natural Systems Engineering, Utah Water Research Laboratory, Utah State University, Logan, 246 p.

Hendrix, N., Criss, A., Danner, E., Greene, C.M., Imaki, H., Pike, A., and Lindley, S.T., 2014, Life cycle modeling framework for Sacramento River winter run Chinook salmon: National Oceanic and Atmospheric Administration Technical Memorandum NOAA-TM-NMFS-SWFSC-530, 30p., accessed October 31, 2017, at https://swfsc.noaa.gov/publications/TM/SWFSC/NOAA-TM-NMFS-SWFSC-530.pdf.

Jager, H.I., 2011, Quantifying temperature effects on fall Chinook salmon: U.S. Department of Energy, Oak Ridge National Laboratory, Oak Ridge, Tennessee, 45 p.

Johnson, C.L., Roni, P., and Pess, G.R., 2012, Parental effect as a primary factor limiting egg-to-fry survival of spring Chinook salmon in the Upper Yakima River Basin: Transactions of the American Fisheries Society, 14, p. 1,295–1,309.

Jones, E.C., Perry, R.W., Risley, J.C., Som, N.A., and Hetrick, N.J., 2016, Construction, calibration, and validation of the RBM10 water temperature model for the Trinity River, northern California: U.S. Geological Survey Open-File Report 2016–1056, 46 p., accessed October 31, 2017, at https://pubs.er.usgs.gov/publication/ofr20161056.

Maunder, M.N., 1997, Investigation of density dependence in salmon spawner–egg relationships using queueing theory: Ecological Modelling, v. 104, no. 2, p. 189–197.

Moussalli, E., and Hilborn, R., 1986, Optimal stock size and harvest rate in multistage life history models: Canadian Journal of Fisheries and Aquatic Sciences, v. 43, no. 1, p. 135–141.

Overstreet, B.T., Riebe, C.S., Wooster, J.K., Sklar, L.S., and Bellugi, D., 2016, Tools for gauging the capacity of salmon spawning substrates: Earth Surface Processes and Landforms, v. 41, no. 1, p. 130–142.

Perry, R.W., Plumb, J.M., and Huntington, C.W., 2015, Using a laboratory-based growth model to estimate mass-and temperature-dependent growth parameters across populations of juvenile Chinook Salmon: Transactions of the American Fisheries Society, v. 144, no. 2, p. 331–336.

Perry, R.W., Risley, J.C., Brewer, S.J., Jones, E.C., and Rondorf, D.W., 2011, Simulating daily water temperatures of the Klamath River under dam removal and climate change scenarios: U.S. Geological Survey Open-File Report 2011–1243, 78 p., accessed October 31, 2017, at https://pubs.usgs.gov/of/2011/1243/.

Plumb, J.M., 2012, Evaluation of models and the factors affecting the migration and growth of naturally-produced subyearling fall Chinook salmon (*Oncorhynchus tshawytscha*) in the lower Snake River: Moscow, University of Idaho, Ph.D. dissertation, 153 p.

Plumb, J.M., and Moffitt, C.M., 2015, Re-estimating temperature-dependent consumption parameters in bioenergetics models for juvenile Chinook salmon: Transactions of the American Fisheries Society, v. 144, no. 2, p. 323–330.

R Core Team, 2015, R—A language and environment for statistical computing: Vienna, Austria, R Foundation for Statistical Computing, accessed October 31, 2017, at https://www.R-project.org/.

Railsback, S.F., Gard, M., Harvey, B.C., White, J.L., and Zimmerman, J.K., 2013, Contrast of degraded and restored stream habitat using an individual-based salmon model: North American Journal of Fisheries Management, v. 33, no. 2, p. 384–399.

Risley, J.C., Brewer, S.J., and Perry, R.W., 2012, Simulated effects of dam removal on water temperatures along the Klamath River, Oregon and California, using 2010 Biological Opinion flow requirements: U.S. Geological Survey Open-File Report 2011–1311, 18 p., accessed October 31, 2017, at https://pubs.usgs.gov/of/2011/1311/.

Rose, K., Anderson, J., McClure, M., and Ruggerone, G., 2011, Salmonid integrated life cycle models workshop—Report of the Independent Workshop Panel, 28 p., accessed October 31, 2017, at http://deltacouncil.ca.gov/sites/default/files/documents/files/Salmonid_ILCM_workshop_final_report.pdf.

Salmon Technical Team, 2005, Klamath River fall Chinook stock-recruitment analysis: Portland, Oregon, Pacific Fishery Management Council, 36 p., accessed October 31, 2017, at https://www.pcouncil.org//bb/2005/1105/G.3.a_Att1_Nov05BB.pdf.

Scheuerell, M.D., Hilborn, R., Ruckelshaus, M.H., Bartz, K.K., Lagueux, K.M., Haas, A.D., and Rawson, K., 2006, The Shiraz model—A tool for incorporating anthropogenic effects and fish–habitat relationships in conservation planning: Canadian Journal of Fisheries and Aquatic Sciences, v. 63, no. 7, p. 1,596–1,607.

Som, N.A., Goodman, D.H., Perry, R.W., and Hardy, T.B., 2015, Habitat suitability criteria via parametric distributions—Estimation, model selection, and uncertainty: River Research and Applications, v. 32, no. 5, p. 1,128–1,137.

Som, N.A., Perry, R.W., Jones, E.C., De Julio, K., Petros, P., Pinnix, W.D., and Rupert, D.L, 2017, N-mix for fish—Estimating riverine salmonid habitat selection via N-mixture models: Canadian Journal of Fisheries and Aquatic Sciences, http://www.nrcresearchpress.com/doi/pdf/10.1139/cjfas-2017-0027.

Stewart, D.J., and Ibarra, M., 1991, Predation and production by salmonine fishes in Lake Michigan, 1978–88: Canadian Journal of Fisheries and Aquatic Sciences, v. 48, no. 5, p. 909–922.

Stewart, D.J., Weininger, D., Rottiers, D.V., and Edsall, T.A., 1983, An energetics model for lake trout, *Salvelinus namaycush*—Application to the Lake Michigan population: Canadian Journal of Fisheries and Aquatic Sciences, v. 40, p. 681–698.

Walters, C., and Korman, J., 1999, Linking recruitment to trophic factors—Revisiting the Beverton–Holt recruitment model from a life history and multispecies perspective: Reviews in Fish Biology and Fisheries, v. 9, no. 2, p. 187–202.

Williamson, S.C., Bartholow, J.M. and Stalnaker, C.B., 1993, Conceptual model for quantifying pre-smolt production from flow-dependent physical habitat and water temperature: River Research and Applications, v. 8, nos. 1–2, p. 15–28.

Zabel, R.W., 2002, Using “travel time” data to characterize the behavior of migrating animals: American Naturalist, v. 159, p. 372–387.

Zabel, R.W., and Anderson, J.J., 1997, A model of the travel time of migrating juvenile salmon, with an application to Snake River spring Chinook salmon: North American Journal of Fisheries Management, v. 17, p. 93–100.

Publishing support provided by the U.S. Geological Survey
Science Publishing Network, Tacoma Publishing Service Center

For more information concerning the research in this report, contact the
Director, Western Fisheries Research Center
U.S. Geological Survey
6505 NE 65th Street
Seattle, Washington 98115
https://wfrc.usgs.gov/

ISSN 2331-1258 (online)
https://doi.org/10.3133/ofr20181056